# OTULIN Antagonizes LUBAC Signaling by Specifically Hydrolyzing Met1-Linked Polyubiquitin

Kirstin Keusekotten,<sup>1,5</sup> Paul Ronald Elliott,<sup>1,5</sup> Laura Glockner,<sup>2</sup> Berthe Katrine Fiil,<sup>3</sup> Rune Busk Damgaard,<sup>3</sup> Yogesh Kulathu,<sup>1</sup> Tobias Wauer,<sup>1</sup> Manuela Kathrin Hospenthal,<sup>1</sup> Mads Gyrd-Hansen,<sup>3</sup> Daniel Krappmann,<sup>2</sup> Kay Hofmann,<sup>4</sup> and David Komander<sup>1,\*</sup>

<sup>1</sup>Medical Research Council Laboratory of Molecular Biology, Francis Crick Avenue, Cambridge, CB2 0QH, UK

<sup>2</sup>Helmholtz Zentrum München, German Research Center for Environmental Health, Research Unit Cellular Signal Integration, Institute of Molecular Toxicology and Pharmacology, Ingolstädter Landstrasse 1, 85764 Neuherberg, Germany

<sup>3</sup>Department of Disease Biology, Novo Nordisk Foundation Center for Protein Research, University of Copenhagen, 2200 Copenhagen, Denmark

<sup>4</sup>Institute for Genetics, University of Cologne, Zülpicher Strasse 47a, 50674 Cologne, Germany

<sup>5</sup>These authors contributed equally to this work

\*Correspondence: dk@mrc-lmb.cam.ac.uk

http://dx.doi.org/10.1016/j.cell.2013.05.014

### SUMMARY

The linear ubiquitin (Ub) chain assembly complex (LUBAC) is an E3 ligase that specifically assembles Met1-linked (also known as linear) Ub chains that regulate nuclear factor κB (NF-κB) signaling. Deubiquitinases (DUBs) are key regulators of Ub signaling, but a dedicated DUB for Met1 linkages has not been identified. Here, we reveal a previously unannotated human DUB, OTULIN (also known as FAM105B), which is exquisitely specific for Met1 linkages. Crystal structures of the OTULIN catalytic domain in complex with diubiquitin reveal Met1-specific Ub-binding sites and a mechanism of substrate-assisted catalysis in which the proximal Ub activates the catalytic triad of the protease. Mutation of Ub Glu16 inhibits OTULIN activity by reducing  $k_{cat}$  240-fold. OTULIN overexpression or knockdown affects NF-κB responses to LUBAC, TNFα, and poly(I:C) and sensitizes cells to TNFα-induced cell death. We show that OTULIN binds LUBAC and that overexpression of OTULIN prevents TNFα-induced NEMO association with ubiquitinated RIPK1. Our data suggest that OTULIN regulates Met1-polyUb signaling.

# INTRODUCTION

Ubiquitination is an important posttranslational modification that regulates diverse processes, including protein degradation, intracellular trafficking, transcription, kinase activation, and the DNA damage response (Hershko and Ciechanover, 1998; Komander and Rape, 2012). This variety of functions is mediated by eight different types of polyubiquitin (polyUb) linkages, and, although the roles of Lys48- and Lys63-linked polyUb have

been studied in great detail, much less is known about the remaining "atypical" Ub chains (Behrends and Harper, 2011; Kulathu and Komander, 2012).

Met1-linked polyUb (Met1-polyUb) is the source of the cellular Ub pool, given that Ub is translated as a polyprotein (Ozkaynak et al., 1984) and posttranslationally processed by dedicated DUBs, such as USP5 (also known as IsoT) (Amerik AYu et al., 1997). This chain type can also be assembled by the linear Ub chain assembly complex (LUBAC), a multisubunit E3 ligase consisting of HOIP, HOIL-1L, and SHARPIN (Gerlach et al., 2011; Ikeda et al., 2011; Kirisako et al., 2006; Tokunaga et al., 2011). LUBAC has roles in NF-κB activation (Haas et al., 2009; Tokunaga and Iwai, 2012; Tokunaga et al., 2009; Walczak et al., 2012) and is required for full activation of the inhibitor of κB (IKB) kinase (IKK) complex. IKK activation leads to the phosphorylation and degradation of  $I\kappa B$  and the activation of the NF- $\kappa B$ transcription factor (Karin and Ben-Neriah, 2000). It is not fully understood how Met1-polyUb regulates this process, but it involves the binding and modification of the IKK subunit NEMO with Met1-linked chains. NEMO harbors a Met1-specific Ubbinding domain (UBD) that is important for NF-κB signaling (Komander et al., 2009; Rahighi et al., 2009).

Much less is known about DUBs that regulate Met1-polyUb chains, and a specific DUB for Met1-linkages has not been identified. Of the roughly 80 active DUBs in the human genome, many show weak or no activity toward Met1-linked chains (Faesen et al., 2011; Komander et al., 2009). A potential reason is the distinct chemistry of a peptide versus an isopeptide linkage (Figure 1A).

Ovarian tumor (OTU) domain DUBs regulate important cell-signaling pathways. A20 regulates NF-κB signaling (Hymowitz and Wertz, 2010), OTUD5 (also known as DUBA) regulates IRF3 signaling (Kayagaki et al., 2007), and OTUB1 regulates the DNA damage response (Nakada et al., 2010). OTU DUBs can be linkage specific. Structural work has revealed the basis for OTUB1 Lys48 specificity (Juang et al., 2012; Wiener et al.,



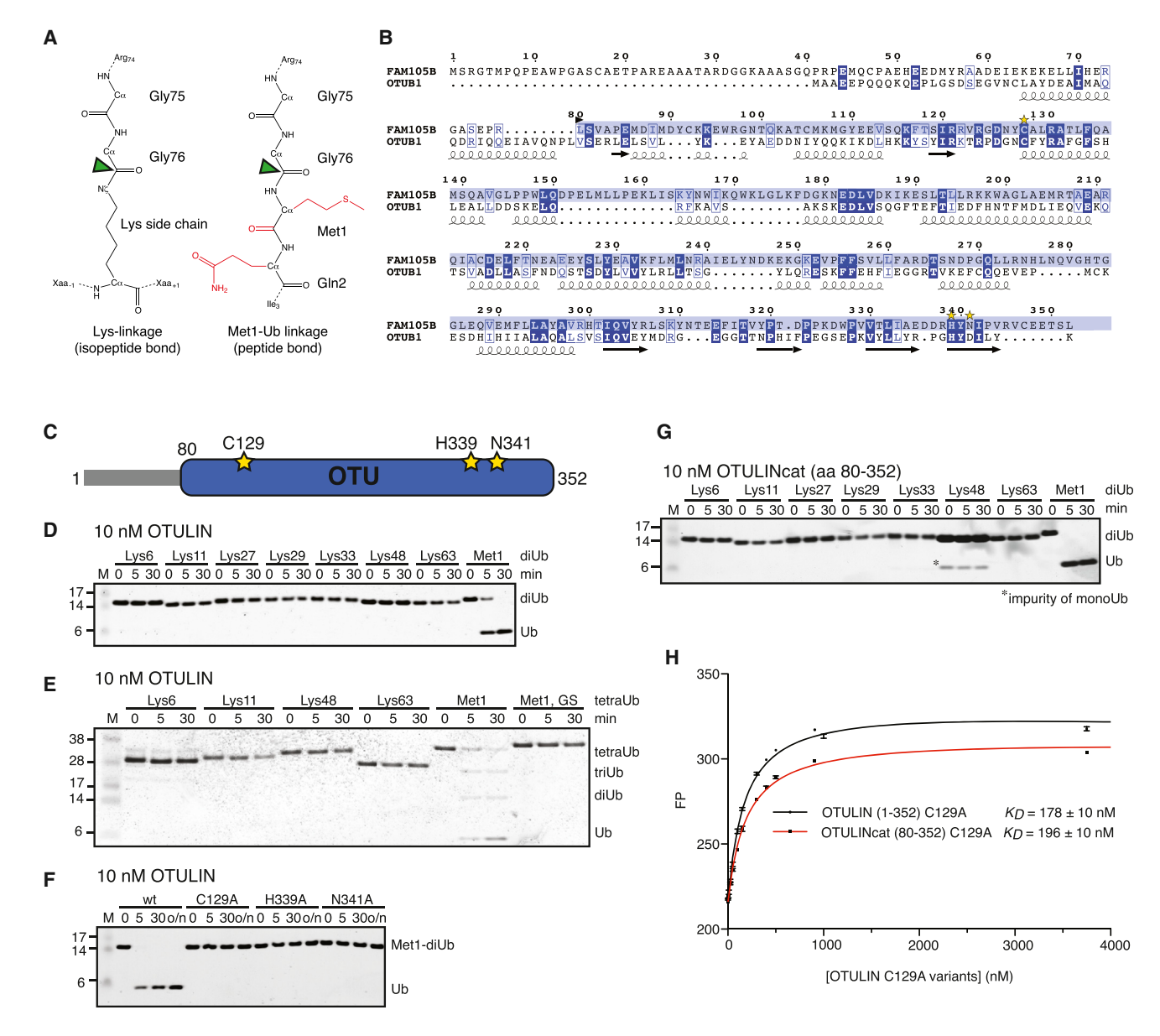
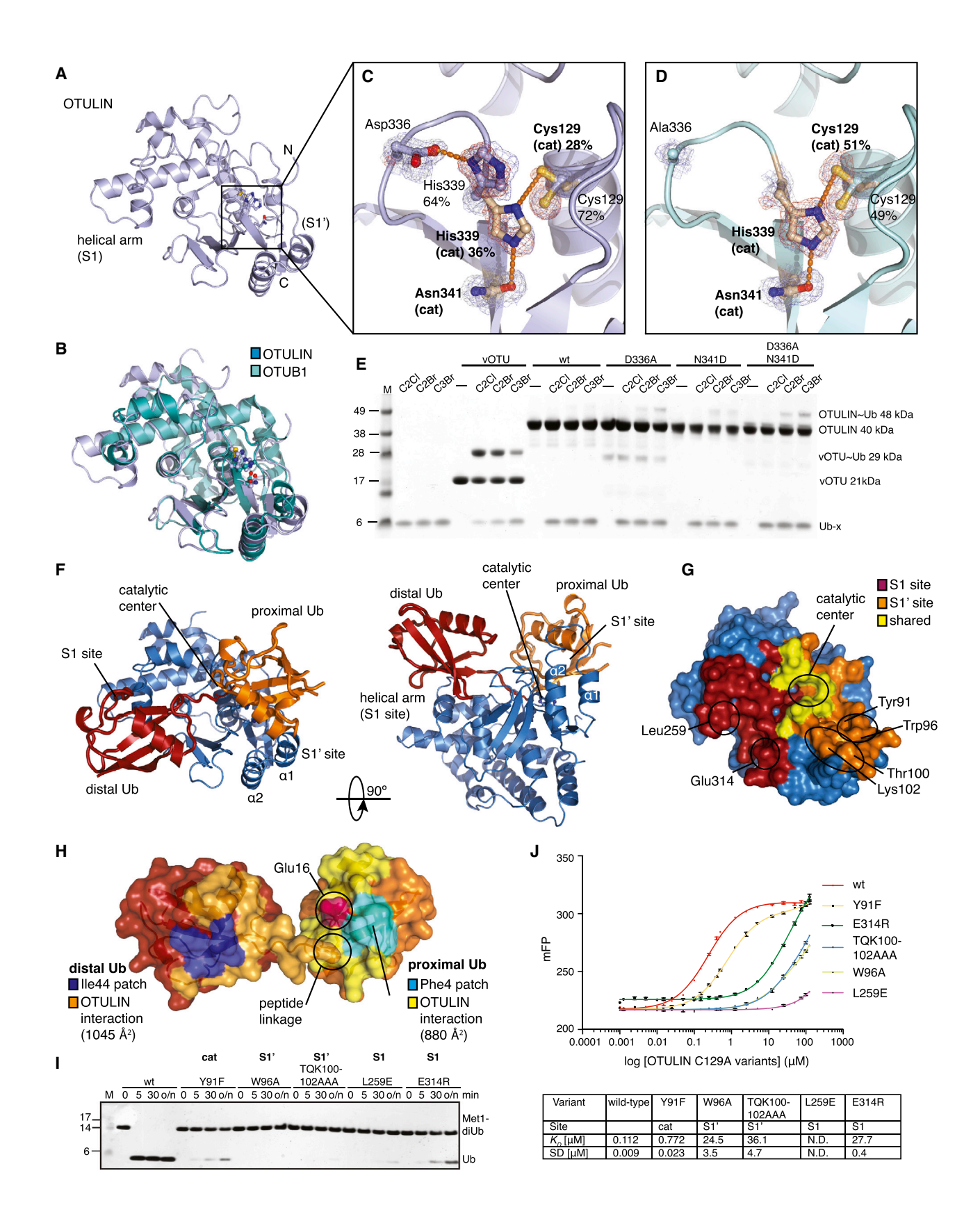


Figure 1. Identification and Specificity of OTULIN

(A) Chemical difference between an isopeptide (left) and Met1-peptide linkage (right) in diUb. The distal Ub (top) is linked via its C-terminal Gly<sup>75</sup>-Gly<sup>76</sup> sequence to a Lys side chain ε-amino group in another Ub or on a substrate, generating a branched peptide. In a Met1-linked chain, the C-terminal Gly76 is connected to Met1 of the distal Ub in a standard peptide linkage. The Met1 and Gln2 side chains, as well as the Met1 carbonyl (red), represent steric differences in comparison to an isopeptide linkage. A green arrow indicates the scissile bond in a DUB reaction.

- (B) Sequence alignment of FAM105B/OTULIN with OTUB1. Sequence identity is 18% for the catalytic domain. Secondary structure elements are shown for OTUB1. The OTU domain is indicated in blue, and catalytic residues are labeled with yellow stars.
- (C) The domain structure of OTULIN colored as in (B).
- (D) Linkage specificity of OTULIN. diUb (1 µM) of all possible linkage types is hydrolyzed over a time course by 10 nM OTULIN and visualized on silver-stained 4%--12% gradient SDS-PAGE gels. See Figure S1D for the assay at 1  $\mu\text{M}$  OTULIN concentration.
- (E) Cleavage of tetraUb chains, as in (D). The last substrate is a Met1-tetraUb with G76S mutation in all Ub moieties.
- (F) Hydrolysis of Met1-diUb by OTULIN wild-type (WT) and catalytic mutants as indicated.
- (G) The OTU domain of OTULIN encodes Met1-linked Ub specificity. diUb specificity analysis as in (D) with OTULIN 80-352 at a 10 nM concentration.
- (H) Affinity measurements by fluorescence anisotropy with OTULIN (1-352) C129A or OTULIN (80-352) C129A and FlAsH-tagged Met1-diUb, as described in the Extended Experimental Procedures. Error bars represent SD from the mean of measurements performed in triplicate.



(legend on next page)

2012) and TRABID specificity against Lys29 and Lys33 linkages (Licchesi et al., 2012). Moreover, viral OTU DUBs have been reported that are highly divergent in sequence but are structurally similar (Frias-Staheli et al., 2007).

Here, we identify a previously unannotated human DUB, FAM105B/OTULIN, which is specific for Met1-linked Ub chains. Structural studies reveal that this specificity is due to Met1-specific Ub-binding sites and a mechanism of substrate-assisted catalysis where a residue in a Met1-linked chain directly participates in the organization of the catalytic triad of the enzyme. Overexpression and knockdown analysis of OTULIN suggest that the protein binds LUBAC and regulates LUBAC-mediated processes in cells.

#### **RESULTS**

# FAM105B/OTULIN, a Met1-Linkage-Specific OTU DUB

Given the high sequence divergence of OTU domains, we set out to identify unstudied OTU enzymes using a bioinformatical screen based on generalized profile analysis (Bucher et al., 1996). Iterative profile refinement, starting from a multiplesequence alignment of experimentally validated OTUs, indicated an OTU domain with a complete catalytic triad in the uncharacterized human protein FAM105B (Figure 1B). FAM105B comprises 352 amino acids (aa), and the OTU domain spans the majority of the protein (aa 80-352) and an N-terminal region with predicted helical content (Figure 1B, 1C). The catalytic domain is highly conserved between species (Figure S1A available online). Bacterially expressed full-length FAM105B did not hydrolyze common fluorescent substrates such as Ub-AMC (Figure S1B). Ub-based suicide inhibitors that comprise an electrophilic group at the Ub C terminus (Borodovsky et al., 2002) covalently modify most OTU domain DUBs but showed no reactivity against FAM105B (Figure S1C). However, DUB assays against diubiquitin (diUb) of all eight linkage types revealed that FAM105B exclusively hydrolyzed Met1-diUb (Figure 1D). The enzyme was active at 10 nM concentration (Figure 1D) and remained Met1 linkage specific at a 1 μM concentration (Figure S1D). Specificity is maintained when longer Ub chains are used as substrates (Figure 1E) but depended on an intact Ub Gly<sup>76</sup>-Met<sup>1</sup> linkage sequence between Ub moieties, given that mutant tetraUb with Ser76-Met1 linkages was not hydrolyzed (Figures 1E and S1E). Catalytic mutants of FAM105B (C129A, H339A, and N341A) did not hydrolyze Met1-diUb (Figure 1F). Having established FAM105B as a Met1-linkage-specific OTU DUB, we named the enzyme OTULIN (OTU DUB with linear linkage specificity). OTULIN is unique, given that the 14 annotated human OTU DUBs cannot hydrolyze Met1-diUb (Mevissen et al., 2013).

# **Molecular Basis for OTULIN Specificity**

Structural studies revealed how OTULIN achieved its unique specificity for Met1 linkages. The catalytic domain of OTULIN (OTULINcat, aa 80-352) is sufficient for linkage specificity (Figure 1G), and OTULINcat C129A bound Met1-diUb with a similarly high affinity as full-length OTULIN C129A, as revealed by fluorescence anisotropy measurements (K<sub>D</sub> 196 versus 178 nM, Figure 1H).

OTULINcat was crystallized, and its structure was determined to 1.3 Å resolution with SeMet phasing (Figure 2A and Table S1). OTULINcat adopts an OTU fold most similar to OTUB1 (rootmean-square deviation [rmsd] 2.1 Å, DALI Z score 8.7) (Figure 2B). Interestingly, catalytic triad residues His339 and Cys129 display two alternate conformations. In the "active" conformation (occupancy ~30%), the catalytic triad is formed by interactions between Asn341, His339, and Cys129 (Figure 2C); e.g., as observed in OTUB1 in complex with Ub suicide inhibitor (Wiener et al., 2012) (Figures S2A-S2C). In the "inhibited" conformation (occupancy ~70%), Asp336 pulls His339 away from its catalytic position (Figure 2C), and Cys129 flips to an inactive rotamer. Next, we determined the structure of OTULIN D336A to 1.35 Å resolution (Figures 2D and S2G and Table S1). There were no global structural perturbations (Figures S2E and S2F), but His339 was now in the active rotamer, and Cys129 showed increased occupancy of the active rotamer (Figure 2D). Consistently, Ub suicide inhibitors that did not modify wild-type (WT) OTULIN modified OTULIN D336A and also OTULIN N341D, in which the catalytic Asn341 was

## Figure 2. Structural Analysis of OTULIN

(A) Structure of OTULINcat (aa 80-352). Ub-binding S1 and S1' sites and termini are indicated. The catalytic center is boxed.

(B) Superposition of OTULIN (blue) and OTUB1 (cyan, PDB 2ZFY) (Edelmann et al., 2009).

(C) A close-up image of the OTULIN catalytic triad (Cys129, His339, and Asn341) showing two alternative conformations for His339 and Cys129. Dotted lines  $indicate \ hydrogen \ bonds. \ A \ simulated \ annealing \ composite \ omit \ map \ (blue, contoured \ at \ 1\sigma) \ and \ |F_o|-|F_c| \ map \ (red, contoured \ at \ 3\sigma) \ is \ shown. \ The \ active \ (beige) \ indicate \ hydrogen \ bonds.$ and inactive (blue) conformation of the catalytic triad are shown. Percentages represent refined occupancies from Refmac5 (Murshudov et al., 2011).

(D) Catalytic center of OTULIN D336A determined at a 1.35 Å resolution (see Figures S2E and S2G) shown as in (C).

(E) OTULIN variants modified by Ub suicide probes, resolved on coomassie-stained SDS-PAGE gels. An 8 kDa shift indicates formation of a covalent OTULIN~Ub

## See Figure S1C and the Extended Experimental Procedures.

(F) Structure of OTULIN (blue) in complex with Met1-diUb (with distal Ub in red and proximal Ub in orange), shown in two orientations. The helical arm comprising the S1 and the  $\alpha$ 1 and  $\alpha$ 2 helices comprising the S1' Ub-binding sites are labeled, and the catalytic center is indicated.

(G) Surface representation of OTULIN showing S1 (dark red), and S1' (orange) binding sites. Yellow indicates residues interacting with both moieties. Labeled residues were mutated for experiments in (I) and (J).

(H) The structure of Met1-diUb indicating the interfaces with OTULIN colored as in (G). The Ile44 patch (blue) of the distal and the Phe4 patch (cyan; Gln2, Phe4, and Thr14) of the proximal Ub is indicated. Ub Glu16<sup>prox</sup> is shown in purple.

(I) Met1-diUb hydrolysis assay performed as in Figure 1D with 10 nM OTULIN and OTULIN Ub-binding mutants. Mutations are annotated accordingly: cat, catalytic and Ub-binding sites; S1 and S1', distal and proximal, respectively.

(J) Affinity (K<sub>D</sub>) measurements of OTULIN C129A with or without Ub-binding mutations performed with fluorescence anisotropy with FIAsH-tagged Met1-diUb (Ye et al., 2011). Error bars represent SD from the mean of measurements performed in triplicate. WT, wild-type; ND, not determined.

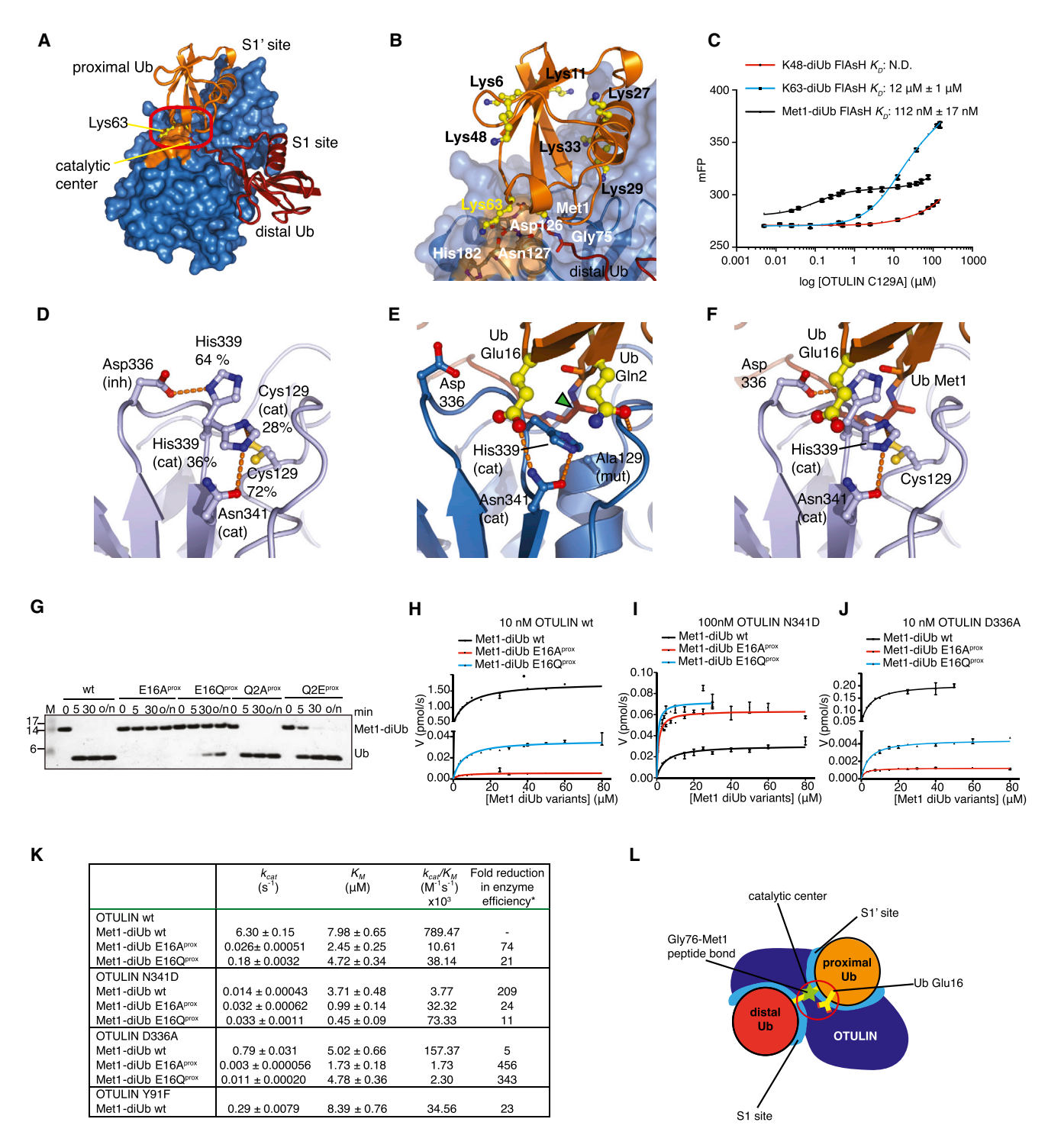


Figure 3. Substrate-Assisted Catalysis in OTULIN

(A) The OTULIN-diUb complex is shown with OTULIN under a blue surface and Met1-diUb colored as red and orange for the distal and proximal moieties, respectively. The catalytic center and Lys63-binding pocket is shown boxed.

<sup>(</sup>B) A close-up view of (A) showing all Ub Lys residues on the proximal Ub (yellow). Lys63 and Met1 are spatially close.

<sup>(</sup>C) Affinity measurements of OTULIN C129A with K48-, K63, and Met1-diUb linkages performed with fluorescence anisotropy (Ye et al., 2011). Error bars represent SD from the mean of measurements performed in triplicate.

<sup>(</sup>D–F) A close-up image of the OTULIN catalytic center showing key residues. Dotted lines indicate hydrogen bonds.

<sup>(</sup>D) Unliganded OTULIN, shown as in Figure 2C.

changed to a negatively charged Asp (Figure 2E). Both mutants stabilize His339 in the active conformation, generating a more reactive enzyme.

To understand how OTULIN acted on Met1-polyUb specifically, we determined the structure of OTULINcat C129A bound to Met1-diUb to 1.9 Å resolution (Figures 2F and S2 and Table S1). The distal and proximal Ub moieties occupy extensive S1 and S1' Ub-binding sites on OTULIN, respectively (Figures 2F-2H). Residues mediating Ub binding are highly conserved in OTULIN orthologs (Figure S2I). The binding interface with the distal Ub covers 1,045 Å<sup>2</sup> and involves the lle44 patch that interacts with a helical arm (aa 254-264) conserved in all OTU domains (Figures 2F-2H). However, compared to the OTUB1~Ub structure (Wiener et al., 2012) (Figure S2J), the distal Ub rotates by  $\sim 18^{\circ}$  in the S1 binding site (Figure S2K). The proximal Ub binds with an interface of 880 Å<sup>2</sup> to an S1' Ub-binding site formed by helices  $\alpha 1$  and  $\alpha 2$  of OTULINcat via an unusual binding surface on Ub involving the Ub helix and the Phe4 patch (Figure 2H). Point mutations in the S1 (L259E and E314R) or S1' (W96A and TQK100-102AAA) Ub-binding sites reduced OTULIN activity toward Met1-diUb (Figure 2I) by decreasing Met1-diUb affinity (Figure 2J).

#### **OTULIN Specificity: Selective diUb Binding**

The extensive S1' Ub-binding site is likely to be important for OTULIN specificity in that it orients the proximal Ub such that only Met1 points toward the catalytic center (Figure 3A). In this orientation of the proximal Ub, all Lys residues are remote from the catalytic center, except for Lys63, which is spatially close to Met1 (Figure 3B). Importantly, OTULIN wedges these linkage points apart by two loops (aa 125-127 and 282-284) that fix Lys63 in a dedicated binding pocket (Figure 3B). Nonetheless, a differently linked Ub chain including a Lys63-linked diUb would rotate the proximal Ub moiety by several degrees, and such orientation would likely not fit the OTULIN S1' binding site. Indeed, Lys63-linked diUb bound with 100-fold reduced affinity (<112 nM for Met1-linked diUb versus 12  $\mu$ M for Lys63-linked diUb), and no binding was detected for Lys48-linked diUb (Figure 3C). This shows that the Ub-binding sites of OTULIN already distinguish between structurally similar Met1 and Lys63 chain types by two orders of magnitude.

# **OTULIN Specificity: Substrate-Assisted Catalysis**

The complex structure revealed that the proximal Ub directly participates in the organization of the catalytic center. Autoinhibition of the catalytic triad in the absence of substrate (Figure 3D) is released by the binding of the Met1-linked proximal Ub (Figures 3E and 3F). The carbonyl group of Met1 sterically interferes with the inhibited conformation of His339, pushing it into an active conformation (Figure 3F). Lys-linked Ub chains lack a structural equivalent of this carbonyl moiety in the linkage (Figure 1A). More significantly, Glu16 of the proximal Ub is inserted into the catalytic center, displacing the inhibitory OTULIN residue Asp336, further restricting the mobility of His339 (Figures 3E and 3F). In addition, Glu16 coordinates the third residue in the catalytic triad Asn341, aligning it toward His339 (Figure 3E).

Importantly, Met1-diUb with mutations of Glu16 in the proximal Ub was hydrolyzed with significantly lower activity in qualitative gel-based assays, whereas mutation of nearby Gln2 (which also interacts with OTULIN, Figure 3E) had no effect (Figures 3G and S3A). All mutants were hydrolyzed by the nonspecific DUB USP21 (Ye et al., 2011) (Figure S3B) and bound to OTULINcat C129A in analytical gel filtration (Figure S3C), and Met1-diUb E16Aprox affinity toward OTULIN C129A was only slightly decreased (612 versus <112 nM, Figure S3D).

We used a quantitative fluorescent kinetic assay for diUb cleavage (Virdee et al., 2010) to examine whether Glu16 on a proximal Ub had a direct role in catalysis (Figures 3H and 3I). Met1-diUb E16A<sup>prox</sup> decreased k<sub>cat</sub> 240-fold and enzyme efficiency  $(k_{cat}/K_M)$  74-fold (because of a 3.5-fold lower  $K_M$  for the mutant) in comparison to Met1-diUb (Figures 3H and 3K). Interestingly, the negative charge on Ub is important for OTULIN activity, given that Met1-diUb E16Qprox still showed a 35-fold lower  $k_{cat}$  for WT OTULIN. Next, we tested whether the more reactive OTULIN N341D or D336A mutants (Figure 2E) showed improved diUb hydrolysis activity. WT Met1-diUb is a poor substrate for OTULIN N341D, most likely because of the repulsion of negative charges (Ub Glu16 and OTULIN Asp341) in the catalytic center (Figures 3I and K). Indeed, OTULIN N341D showed improved kinetics when Ub Glu16 was mutated, and both  $k_{cat}$  and  $K_{M}$ improved, although WT activity was not regained. The OTULIN N341D mutant worked best with Met1-diUb E16Q<sup>prox</sup>, suggesting that the requirement for a negative charge was partially compensated (Figures 3J and 3K). The coordination of Asn341 is a key event in OTULIN activation, as was confirmed when the only OTULIN residue coordinating the Asn341 side chain, Tyr91, was mutated to Phe, resulting in 20-fold reduction of  $k_{cat}$  while not affecting  $K_M$  (Figures 2I, 2J, 3K, and S3F). Strong effects of Glu16 mutation were also observed in the OTULIN D336A mutant (Figures 3J and 3K). Altogether, this showed that the coordination of the catalytic triad through Ub interaction is important for OTULIN activation (Figure 3L).

Hence, we reveal a mechanism of substrate-assisted catalysis in which Glu16 of the proximal Ub activates the catalytic triad of OTULIN by both restricting the movement of the catalytic His339 and introducing a negative charge, presumably for the proper

<sup>(</sup>E) OTULIN C129A (blue) in complex with Met1-diUb (red and orange). Residues from the proximal Ub are shown in yellow. A green arrow indicates the scissile bond (compare to Figure 1A).

<sup>(</sup>F) Superposition of (D) with the Met1-diUb from (E). The carbonyl of Met1 and the side chain of Glu16 of the proximal Ub disengage the autoinhibition of His339. Gln2 is omitted for clarity.

<sup>(</sup>G) OTULIN hydrolysis of Met1-diUb mutated in the proximal moiety performed as in Figure 1D. o/n, overnight incubation.

<sup>(</sup>H–J) Kinetic parameters of OTULIN variants measured by fluorescence anisotropy. Initial rates of hydrolysis at varying substrate concentrations containing 150 nM FIAsH-tagged Met1-diUb variants were fitted to the Michaelis-Menten kinetic model with GraphPad Prism 5. Error bars represent SDs from the mean of measurements performed in triplicate.

<sup>(</sup>K) Summary of kinetic parameters measured. \*, fold reduction in enzyme efficiency relative to OTULIN WT + Met1-diUb WT.

<sup>(</sup>L) A schematic representation of OTULIN mechanism, which involved extensive S1 and S1' sites and substrate-assisted catalysis mediated by Ub Glu16.

coordination of Asn341 for catalysis. OTULIN's usage of a catalytic Asn improves interaction with Glu16 containing Met1-linked chains.

It appears that OTULIN has evolved Met1-linkage-specific Ub-binding sites to specifically interact with linear chains. Additionally, to further distinguish chain types, OTULIN invokes a mechanism of substrate-assisted catalysis in order to ensure that only Met1 linkages are hydrolyzed. OTULIN's remarkable specificity suggests that Met1-linked polyUb have to be tightly regulated independently of other ubiquitination events in cells.

# **Cellular OTULIN Antagonizes LUBAC Signaling**

The identification of OTULIN as a Met1-linkage-specific DUB prompted us to study its role in cells. The human FAM105B gene is ubiquitously expressed (http://biogps.org/%23 goto%3Dgenereport%26id%3D90268). A polyclonal antiserum detected OTULIN in human embryonic kidney (HEK) 293ET and other cell lines (Figure S4A–S4C). C-terminal GFP-tagged OTULIN is cytoplasmic, active, and Met1 specific (Figure S4D–S4F). OTULIN is evolutionarily restricted to vertebrates and selected invertebrate lineages but is not detected in D. melanogaster and C. elegans. Interestingly, all OTULIN-comprising taxa also contain genes for components of the Met1-polyUb chain assembly machinery LUBAC.

Expression of the LUBAC components HOIP, HOIL-1L, and SHARPIN induced Met1-polyUb, which was removed when OTULIN was coexpressed (Figure 4A, lanes 2 and 3). Inactive OTULIN C129A led to the significant enrichment of Met1-polyUb in cells, and OTULIN Ub chain-binding mutants W96A and L259E (Figures 2I and 2J) increased Met1 linkages in cells, albeit not to the same extent as C129A (Figure 4A, lanes 4–6).

Expression of LUBAC induces NF- $\kappa$ B activation (Gerlach et al., 2011; Ikeda et al., 2011; Tokunaga et al., 2009), which was suppressed when OTULIN was transiently coexpressed (Figure 4B) and also in stable cell lines overexpressing OTULIN (Figures S4G and S4H). Despite the enrichment of Met1-polyUb (Figure 4A), OTULIN catalytic or Ub-binding mutants still inhibited LUBAC-driven NF- $\kappa$ B activity to some extent (Figure 4B). Apparently, the increase in Met1-polyUb alone is not sufficient to augment NF- $\kappa$ B activity (Figures 4A and 4B).

NF- $\kappa$ B activation by TNF $\alpha$  leads to the translocation of the cytosolic p65 NF- $\kappa$ B subunit to the nucleus (Hayden and Ghosh, 2008) (Figures 4C, S5C, and S5D). Transient overexpression of OTULIN or OTULIN C129A blocked p65 nuclear translocation after TNF $\alpha$  stimulation, whereas OTULIN W96A or OTULIN L259E had no effect (Figures 4C, S5C, and S5D). It appears that OTULIN overexpression antagonizes NF- $\kappa$ B activation by removing Met1-polyUb, whereas OTULIN C129A acts as a high-affinity UBD that competes with other Met1-specific UBDs required for NF- $\kappa$ B signaling in a similar manner to the one recently reported for the overexpression of the NEMO UBAN domain (van Wijk et al., 2012).

These results suggested that OTULIN was able to regulate LUBAC mediated processes in cells. One of the few reported targets of LUBAC is NEMO (Tokunaga et al., 2009). Transfection of GST-tagged NEMO resulted in NEMO modification which was prevented in a NEMO K285/309R double mutant where

ubiquitination sites are mutated (Tokunaga et al., 2009) (Figure 4D). Co-overexpression of LUBAC resulted in an additional Ub band on NEMO, and the Met1-specific antibody indicated that this additional band was a short Ub chain. This was absent in OTULIN-overexpressing stable cell lines (Figures 4D and S5F) suggesting that OTULIN could remove Met1-polyUb from NEMO.

Glutathione S-transferase (GST) pulldown of NEMO precipitated HOIP, HOIL1, SHARPIN, and OTULIN, suggesting that these proteins might form a complex (Figures 4D and S5F). Immunoprecipitation (IP) of endogenous SHARPIN precipitated endogenous HOIP and, interestingly, also endogenous OTULIN under unstimulated conditions (Figures 4E and S5G). Upon TNF $\alpha$  stimulation, the TNF-R1 was enriched in SHARPIN IPs (Figure 4E), further supporting the idea that a LUBAC-OTULIN complex is formed and that this complex may translocate to the TNF receptor signaling complex (TNF-RSC).

Met1-linked polyUb is known to affect complex assembly at the TNF-RSC (Haas et al., 2009). IP of endogenous NEMO coprecipitates ubiquitinated RIPK1 after TNF $\alpha$  stimulation. Importantly, overexpression of OTULIN abrogated NEMO-RIPK1 complex formation (Figure 4F). This supports the idea that the interaction between NEMO and RIPK1 is stabilized by Met1 linkages and reveals a mechanism of how OTULIN may affect NF- $\kappa$ B activation in response to TNF $\alpha$  stimulation.

## **Ubiquitin Glu16 Is Important for Met1-polyUb Signaling**

Next, with a cellular readout for OTULIN overexpression at hand, we set out to test OTULIN's mechanism of substrate-assisted catalysis in cells by characterizing the effects of an Ub E16A mutant. Control experiments assessing whether this mutant is still assembled in Met1-polyUb by HOIP gave the surprising result that a minimal HOIP ligase construct (Smit et al., 2012; Stieglitz et al., 2012) was impaired in assembling Met1-linked chains from Ub E16A (Figure 5A). Furthermore, fluorescent Met1-diUb E16A<sup>prox</sup> bound to the NEMO UBAN domain with reduced affinity (Figure 5B), which is consistent with the known interaction between the NEMO UBAN domain and Ub Glu16 (Figure 5C) (Rahighi et al., 2009).

Despite this, co-overexpression of Ub E16A and LUBAC in HEK 293ET cells still activated NF- $\kappa$ B, and this could not be completely reversed by OTULIN (Figure 5D), consistent with OTULIN's inability to efficiently hydrolyze Ub E16A-containing polymers (Figure 3). These results suggested that Ub Glu16 is important in multiple aspects of Met1-polyUb signaling.

#### **OTULIN Affects LUBAC-Mediated Cytokine Responses**

Transient overexpression of OTULIN or the well-studied NF- $\kappa$ B inhibitor A20 (Hymowitz and Wertz, 2010) blocks poly(I:C) induced NF- $\kappa$ B activity (Figure 6A). In comparison, OTULIN inhibits TNF $\alpha$ -mediated NF- $\kappa$ B by  $\sim$ 50%, which correlates with effects observed by LUBAC downregulation (Haas et al., 2009; Tokunaga et al., 2009) (Figure 6A). In OTULIN-expressing stable cell lines, transcription of NF- $\kappa$ B target genes was reduced in response to 10 ng/ml TNF $\alpha$  (Figure 6B), and, although I $\kappa$ B $\alpha$  was rapidly phosphorylated and almost completely degraded after 15 min of TNF $\alpha$  stimulation in control cell lines, I $\kappa$ B $\alpha$  phosphorylation, degradation, and NF- $\kappa$ B activation was delayed in

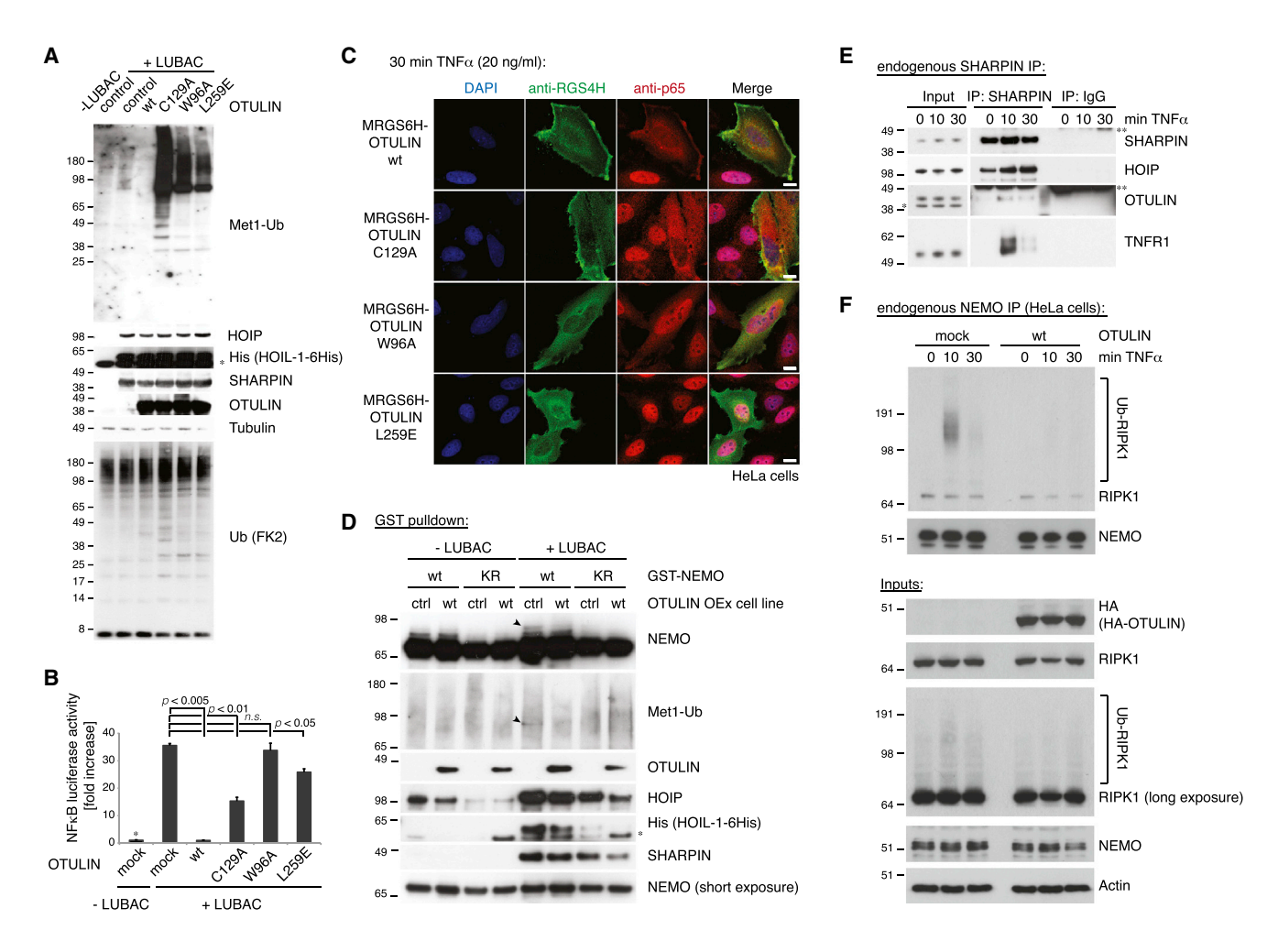


Figure 4. Cellular Functions of OTULIN

(A) HEK 293ET cells were transfected with plasmids for LUBAC and indicated OTULIN variants (see the Extended Experimental Procedures), and lysates were analyzed by western blotting with the indicated antibodies, including the Met1-linkage-specific antibody (Matsumoto et al., 2012).

(B) NF-κB luciferase assays in HEK 293ET cells for the experiment shown in (A). Error bars represent SD from the mean of experiments performed in triplicate. p values are given to indicate significance. \*, mean value set to 1; n.s., nonsignificant.

(C) HeLa cells were transiently transfected with indicated plasmids, treated with TNFa (20 ng/ml) for 30 min, and analyzed by immunofluorescence with indicated antibodies (see Figure S5 for controls and quantification). The scale bar represents 10 μm.

(D) Pulldown of GST-tagged NEMO wild-type (WT) or K285/309R (KR), with or without LUBAC, in control or OTULIN-overexpressing T-REx 293 cell lines. Western blotting with indicated antibodies reveals polyUb on NEMO (arrowhead), which is lost when OTULIN is coexpressed. See also Figure S5.

(E) Immunoprecipitation (IP) of endogenous SHARPIN coprecipitates HOIP and OTULIN and after TNFα stimulation (100 ng/ml), also TNFR1 is shown as revealed by western blotting with the indicated antibodies. \*, nonspecific band; \*\*, heavy chain. See also Figure S5.

(F) IP of endogenous NEMO coprecipitates polyubiquitinated RIPK1 (Ub-RIPK1) after TNFα stimulation (10 ng/ml) of HeLa cells. Western blotting with the indicated antibodies reveals that transient OTULIN overexpression prevents this complex formation.

OTULIN-overexpressing cells (Figure 6C). Moreover, stable overexpression of OTULIN sensitized cells to TNFα-induced cell death (Figures 6D and 6E), consistent with observations in cpdm mice that lack Sharpin (Gerlach et al., 2011; Ikeda et al., 2011; Tokunaga et al., 2011; Walczak et al., 2012) or in humans with mutations in HOIL1 (Boisson et al., 2012). OTULIN overexpression promoted enhanced and persistent JNK activation and c-Jun phosphorylation at later time points, leading to the cleavage of PARP and caspase-3, two key players in the regulation of cell-death induction (Figure 6F). As for  $I\kappa B\alpha$  phosphorylation, OTULIN overexpression also resulted in a delay of JNK activation kinetics (Figures 6C and 6F).

Small interfering RNA (siRNA) against OTULIN resulted in an increase in LUBAC-induced NF-κB activation in HEK 293ET and U2OS cells and also in T-REx 293 cells stably expressing a doxycycline-inducible OTULIN-targeting microRNA (miRNA) (Figures 7A and S6A-S6C). LUBAC-dependent induction of NF-κB could be prevented by co-overexpression of

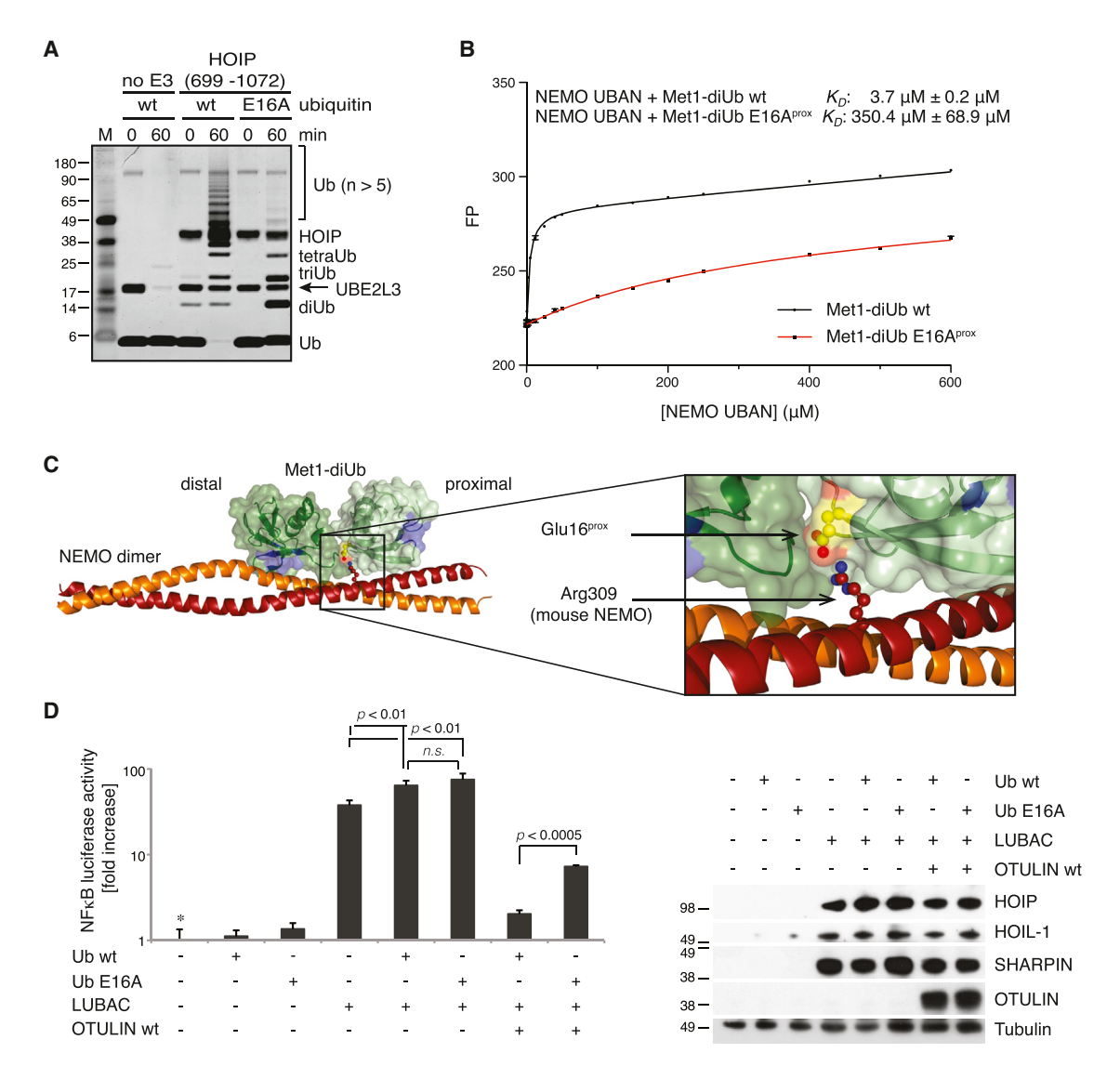


Figure 5. Importance of Ub Glu16 for Met1-polyUb Biology

(A) A minimal HOIP construct (aa 699–1072) that efficiently assembles Met1-Ub chains with WT Ub (Smit et al., 2012; Stieglitz et al., 2012) is less efficient with Ub E16A<sup>prox</sup> in vitro. A silver-stained SDS-PAGE gel is shown.

(B) Fluorescence anisotropy of NEMO UBAN domain binding to FlAsH-tagged Met1-diUb and Met1-diUb E16A<sup>prox</sup>. The UBAN domain binds the mutant Ub chain with ~100-fold lower affinity. Error bars represent SD from the mean from triplicate measurements.

(C) Structural basis for decreased affinity of NEMO for Met1-diUb E16A<sup>prox</sup> mutant. The structure of the NEMO UBAN domain dimer (orange) bound to Met1-diUb is shown (PDB 2ZVN [Rahighi et al., 2009], one diUb omitted for clarity). Ub molecules are shown under a green surface with lle44 hydrophobic patches in blue. Glu16 and its interacting residue Arg309 (mouse NEMO, corresponding human residue Arg312) are shown in stick representation. The inset highlights this interaction. Glu16<sup>prox</sup> also bridges the two Ub moieties and interacts with the C terminus of a distal Ub (data not shown).

(D) Luciferase assays performed as in Figure 4B for HEK 293ET cells transfected with or without LUBAC, WT OTULIN, and Ub WT or Ub E16A. p values are given to indicate significance.\*, mean value set to 1; n.s., nonsignificant. Input levels of transfected proteins, analyzed by western blotting with the indicated antibodies, are shown on the right.

active, but not inactive, OTULIN (Figure 7A). Interestingly, western blotting against the overexpressed LUBAC components revealed that HOIP was ubiquitinated in OTULIN miRNA cell lines (Figure 7B), and coexpression of OTULIN removed these chains, showing that they are Met1 linked (Figure 7B). This suggested that one role of OTULIN in the LUBAC complex (Figure 4E) is to prevent the autoubiquitination of HOIP. However, LUBAC recruitment to the TNF-RSC was unchanged in

OTULIN knockdown cell lines, and Met1-Ub linkages were enriched in the TNF-RSC, implying that OTULIN also regulates Met1-Ub on other components (Figure 7C). Accordingly, we observed a slight increase in RIPK1 ubiquitination enriched with a Met1-linkage-specific Ub-binding matrix in OTULIN-depleted U2OS cells (Figure 7D), suggesting that RIPK1 Met1 ubiquitination in response to TNF $\alpha$  is targeted by OTULIN (Figure 4F).

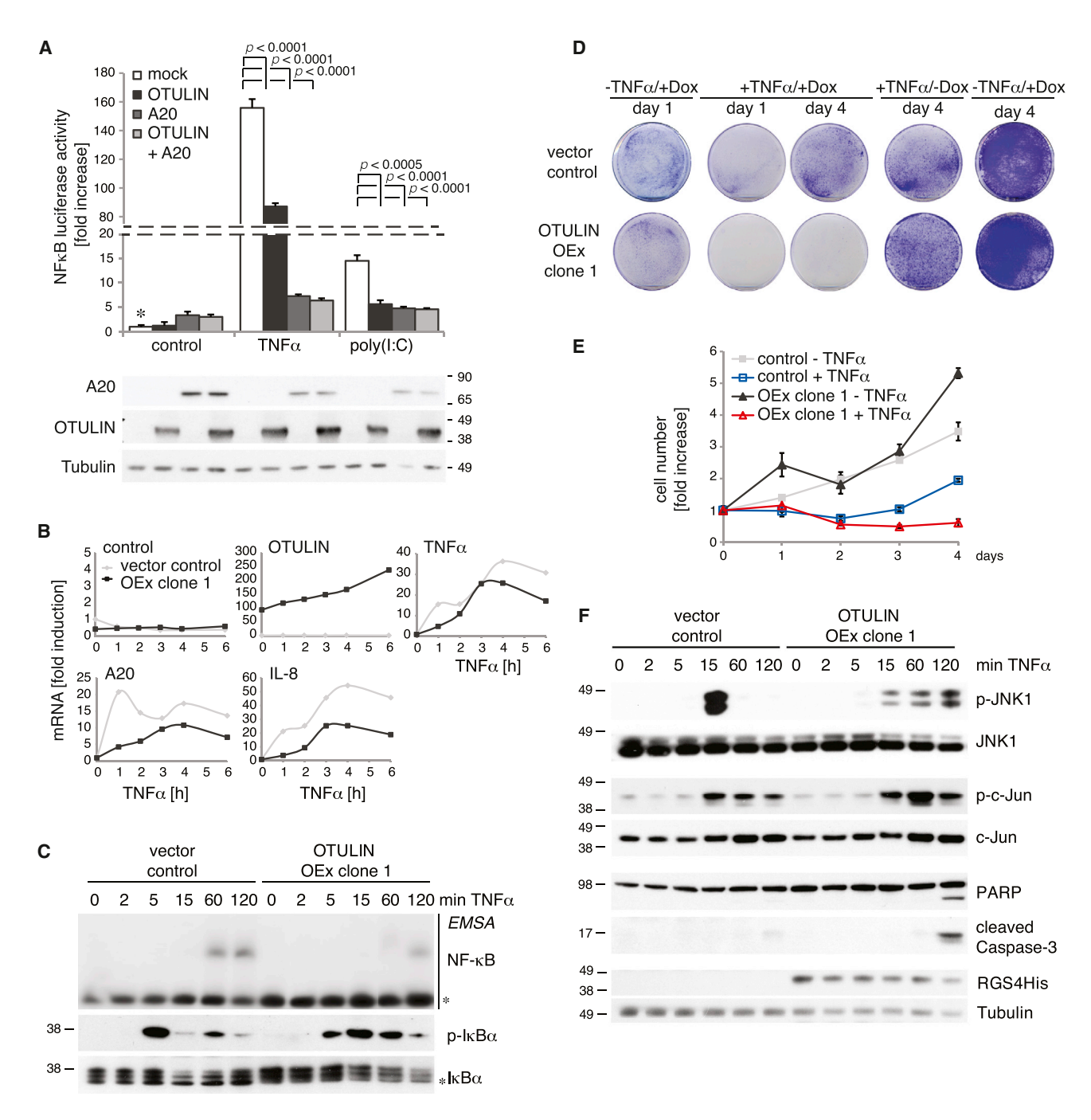


Figure 6. OTULIN Overexpression Inhibits TNFα Signaling

(A) Luciferase assays performed as in Figure 4B in HEK 293ET cells transfected with OTULIN, A20, or both OTULIN and A20 and stimulated with TNFa (100 ng/ml) or poly(I:C) (10 µg/ml). Western blots below show transfected protein levels. Error bars represent SD from the mean for experiments performed in triplicate. p values are given to indicate significance. \*, the control set to 1.

(B–F) Stable doxycycline-inducible control and OTULIN-overexpressing T-REx 293 cells after treatment with 1 μg/ml doxycyclin (Dox) for 24 hr (see the Extended Experimental Procedures).

- (B) Quantitative PCR (qPCR) analysis of selected NF-κB target genes in control (gray) and OTULIN-overexpressing cells (black) after treatment with 10 ng/ml TNF $\alpha$  for the indicated times.
- (C) Analysis of TNFα-stimulated NF-κB activation and IκBα phosphorylation upon TNFα treatment (100 ng/ml) over the indicated time course by western blotting with indicated antibodies and EMSA. See (F) for tubulin control.
- (D) Clonogenic survival of indicated cell lines ± Dox and ± TNFα (50 ng/ml) for 24 hr (see the Extended Experimental Procedures).
- (E) Cell viability counts of cells treated as in (D). Error bars represent SD from the mean for experiments performed in triplicate.
- (F) Analysis of TNFα-stimulated signaling cascades upon TNFα treatment (100 ng/ml) over the indicated time course by western blotting.

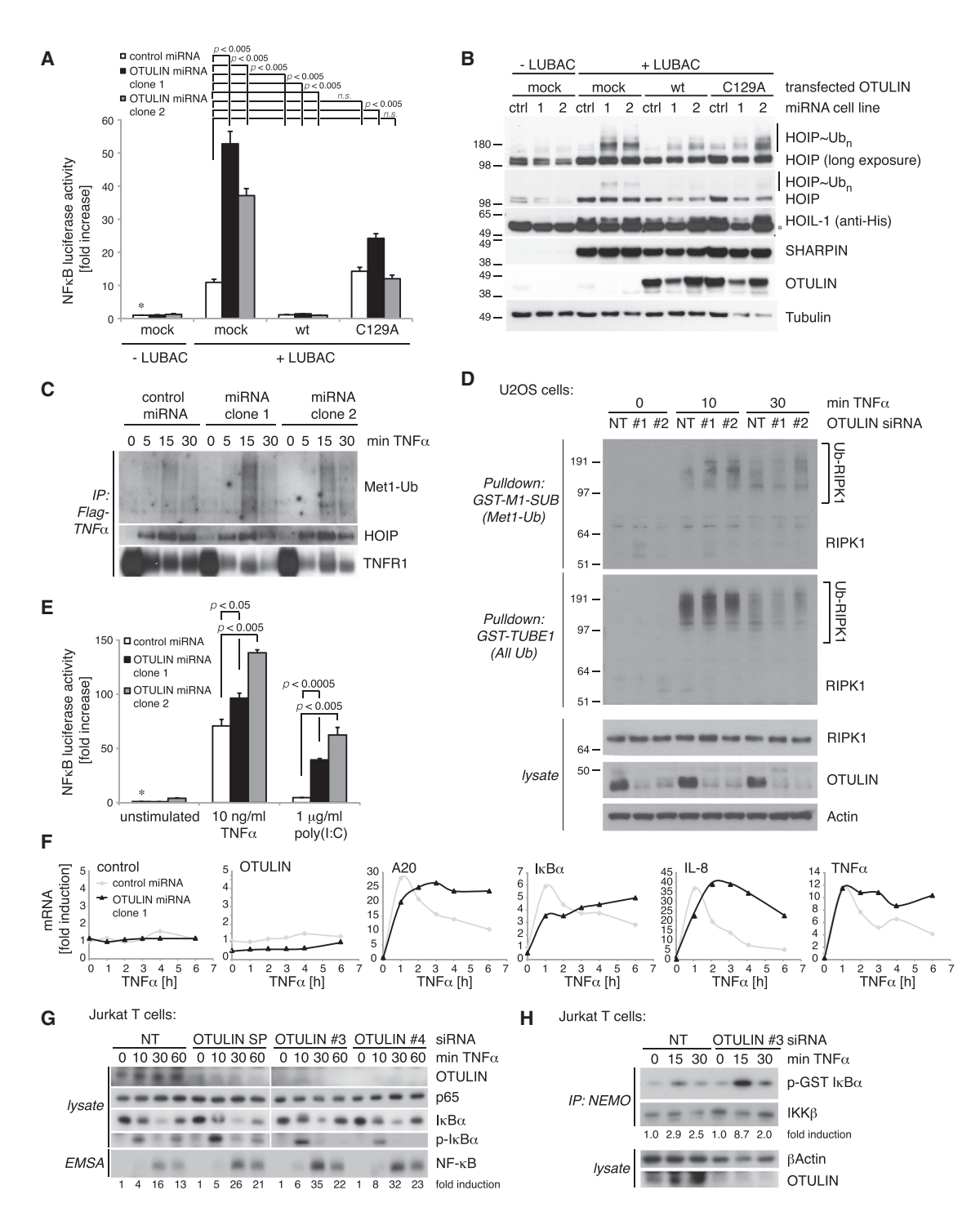


Figure 7. OTULIN Depletion Amplifies LUBAC Signaling

(A-C, E-F) Experiments in stable T-REx 293 cell lines inducibly expressing control or OTULIN-targeting miRNA (see Experimental Procedures and Figure S6).

(A) NF-κB luciferase activity shown as in Figure 4B in cells transfected with LUBAC and indicated OTULIN variants. Error bars represent SD from the mean of experiments performed in duplicate. p values are given to indicate significance. \*, the control set to 1; n.s., nonsignificant.

(B) Western blotting analysis of lysates from (A) with indicated antibodies. \*, nonspecific band.

(C) Immunoprecipitation of the TNF-RSC by FLAG-TNFα (100 ng/ml) from control and OTULIN-depleted cell lines at indicated time points western blotted against Met1-polyUb, HOIP, and TNFR1.

(D) Met1-Ub-specific GST-M1-SUB or general GST-TUBE1 Ub pulldown from U2OS cells stimulated with TNFα (10 ng/ml) after transfection of OTULIN siRNA or a nontargeting (NT) control siRNA.

(legend continued on next page)

Stable OTULIN knockdown affected cytokine responses and led to enhanced NF- $\kappa$ B activation after poly(I:C) and TNF $\alpha$  (Figure 7E), and, even though the initial induction of NF-κB target genes was not severely altered after OTULIN knockdown, expression of A20,  $I\kappa B\alpha$ , IL-8, and  $TNF\alpha$  was sustained in response to TNFα (Figure 7F). Initial phosphorylation and degradation of  $I\kappa B\alpha$  after TNF  $\!\alpha$  stimulation was only slightly enhanced in OTULIN knockdown cells (Figure S6D). However, JNK and c-Jun phosphorylation was sustained at late time points, again leading to cell death (Figures S6D-S6F). The fact that both overexpression and knockdown of OTULIN led to cell death was surprising and requires further investigation.

OTULIN knockdown cell lines were deregulated in their NF-κB response, but we could not observe a strong effect on canonical NF-κB signaling. Jurkat cells express higher amounts of OTULIN (Figure S4C), and OTULIN knockdown by siRNA led to an increase in phospho-I $\kappa$ B $\alpha$  and subsequent enhancement of NF-κB DNA binding (Figure 7G). This was due to increased IKK activation (Figure 7H), consistent with current models of LUBAC function (Tokunaga and Iwai, 2012; Walczak et al., 2012). Altogether, our data are consistent with a role of OTULIN in LUBAC-mediated Met1-polyUb signaling.

# **DISCUSSION**

Here, we identify FAM105B/OTULIN as a human OTU DUB specific for Met1-linked Ub chains. OTULIN is a missing piece in Met1-Ub chain biology, for which no linkage-specific DUB has been described to date. Our data suggest that OTULIN is an antagonist of LUBAC in vitro and in cells. We reveal the molecular basis for the remarkable Met1 linkage specificity by structural and biophysical studies and give insights into potential roles of OTULIN as a LUBAC interactor and antagonist in cells. Consistent with the biochemical findings, overexpression of OTULIN removes Met1-polyUb and dampens LUBAC-mediated NF-κB signaling, whereas knockdown of OTULIN leads to increased Met1-polyUb, IKK activation, and NF- $\kappa$ B signaling after TNF $\alpha$ stimulation. However, both overexpression and knockdown of OTULIN sensitized cells to TNFα-induced cell death, suggesting more complex roles for Met1 linkages in balancing signaling pathways downstream of the TNF $\alpha$  receptor.

# Structural Insights into Ub Chain Linkage Specificity in **DUBs**

Linkage specificity in DUBs is not well understood, and the structure of apo OTULIN did not explain its Met1 specificity, because of its structural similarity to the Lys48-specific OTUB1. The key insight into linkage specificity for these two enzymes came from the complex structures of the enzyme with two Ub molecules bound across the active site.

A high-affinity Ub-binding site in OTULIN allows it to select Met1-linked chains with 100-fold preference over Lys63 linkages and disallows the binding of Lys48-linked and presumably other chains. This mechanism is shared by many DUBs; e.g., TRABID (Licchesi et al., 2012) and OTUB1 (Juang et al., 2012; Wiener et al., 2012). However, in a physiological situation where multiple Ub chain linkages are often mixed, substrate-targeted DUBs may cleave additional Ub chain types. OTULIN prevents such promiscuity by requiring a properly positioned Ub residue, Glu16, for catalytic efficiency. Even in Lys63-linked chains, the required rotation of the proximal Ub would displace Ub Glu16, preventing activity. Therefore, OTULIN is the first DUB for which substrate-assisted catalysis has been demonstrated to achieve linkage specificity. It is possible that substrate-assisted catalysis explains the linkage (or substrate) specificity of other DUBs. It will also be interesting to see whether DUB activators exist that complement the catalytic triad in an analogous manner as that observed in OTULIN.

Ub-mediated substrate-assisted catalysis was recently shown to be crucial for the assembly of Lys11-linked polyUb, where Ub Glu34 complements the active site of the E2 Ub-conjugating enzyme UBE2S (Wickliffe et al., 2011). The fact that Glu16 also impairs HOIP activity also suggests the functionality of this side chain in assembly reactions. Altogether, this shows that Ub is more than just a binding partner for other proteins and that it can actively participate in enzymatic reactions.

# **Cellular Role of OTULIN in Counteracting LUBAC**

In transfection experiments, we demonstrated that OTULIN could counteract cellular LUBAC responses, suggesting that OTULIN helps to balance the amount of Met1-polyUb in cells. Furthermore, the mechanism of substrate-assisted catalysis suggests that OTULIN may not target individual proteins but, instead, target Met1-linked Ub chains, regardless of where they are attached. Indeed, we identified three proteins that change in their ubiquitination status when OTULIN levels are modulated. NEMO and RIPK1 are among the few reported targets of LUBAC (Gerlach et al., 2011; Tokunaga et al., 2009).

We provide evidence that OTULIN directly interacts with LUBAC. The observation that depletion of OTULIN leads to the modification of HOIP with Met1-polyUb suggests that HOIP, like many other E3 ligases, undergoes autoubiquitination and that OTULIN has the ability to prevent this. This most likely explains why the overexpression of OTULIN chain-binding mutants lead to increased Met1-polyUb in cells (Figure 4A). Moreover, this interaction most likely recruits OTULIN to LUBAC targets. However, the functional consequences of a LUBAC-OTULIN interaction are unclear, given that HOIP stability, recruitment, and activity appear to be unaffected, and this requires further investigation.

<sup>(</sup>E) NF-κB luciferase activity in control and OTULIN-depleted cell lines after treatment with TNFα (10 ng/ml) or poly(I:C) (1 μg/ml). Error bars represent SD from the mean of experiments performed in duplicate. p values are given to indicate significance. \*, the control set to 1; n.s., nonsignificant.

<sup>(</sup>F) Analysis of selected NF-κB target genes by qPCR in control and OTULIN-depleted cell lines over a time course of TNFα stimulation (10 ng/ml).

<sup>(</sup>G) Jurkat cells transfected with nontargeting (NT) control siRNA or three different OTULIN-specific siRNAs were treated with TNFα (25 ng/ml) as indicated. EMSA signals were quantified by densitometry. SP, smart pool.

<sup>(</sup>H) OTULIN or control siRNA-transfected Jurkat cells were stimulated for 15 and 30 min with TNFα (25 ng/ml). After NEMO IP, kinase assays were performed with GST- $l\kappa B\alpha$  (aa 1–53) as a substrate and quantified by densitometry.

Regarding the functional requirement for Met1-linked chains in NF-κB responses, key questions remain to be answered. First, in contrast to Lys63-linked chains, for which roles in NF-κB signaling have long been verified, for example, by elegant replacement strategies (Xu et al., 2009), Met1-linked polymers have a very low abundance, and are hard to detect in cell lysates. This may change with the discovery that catalytically inactive OTULIN (Figure 4A) or OTULIN knockdown (Figure 7C) leads to the stabilization of Met1 linkages. A second, more important issue is the lack of proteins modified with Met1-polyUb in vivo after a physiological stimulus. We believe that OTULIN can also be instrumental here, given that its specificity can be exploited as a Met1-specific Ub-binding protein when inactivated or in mass spectrometry methods. We anticipate that the identification of LUBAC and OTULIN targets may reveal a surprising variety of cellular proteins not restricted to NF-κB signaling.

# **Role of OTULIN in Cytokine Responses**

Our data identify roles of OTULIN in TNF $\alpha$  signaling, which is in agreement with reported roles of Met1-polyUb in this pathway (Haas et al., 2009; Tokunaga et al., 2009; Walczak et al., 2012). However, in TNF $\alpha$  signaling, the putative redundant or nonredundant involvement of many different Ub chain types leads to a complicated interplay of Ub signaling (Kulathu and Komander, 2012). The functional importance of Met1-linked chains in the mix is supported by genetic evidence from cpdm mice lacking SHARPIN (Gerlach et al., 2011; Ikeda et al., 2011; Tokunaga et al., 2011) and data from human patients with mutations in HOIL1 (Boisson et al., 2012). So far, there is no unifying molecular mechanism that explains why so many different forms of polyUb are seemingly important for the activation of identical kinase cascades upon TNF $\alpha$  stimulation. Interestingly, the effects of OTULIN overexpression or knockdown seem more pronounced in poly(I:C) versus TNFα signaling (Figures 6A and 7E), and it will be important to study roles of OTULIN in other pathways that depend on Met1-linked chains, such as NOD2 signaling (Damgaard et al., 2012).

Our data support a role of Met1 linkages in providing an important scaffold for productive complex formation, given that the loss of Met1-linked chains induced by OTULIN overexpression prevents the association of NEMO with ubiquitinated RIPK1. Ubiquitinated RIPK1 is targeted also by the DUBs A20 (Hymowitz and Wertz, 2010) and CYLD (Sun, 2010). CYLD hydrolyzes Met1 linkages (Komander et al., 2009) and, hence, could also contribute to antagonize LUBAC signaling. However, although A20 and CYLD are induced by  $\mathsf{TNF}\alpha$  for the establishment of a negative feedback loop, neither OTULIN (Figure 7F) nor LUBAC (Haas et al., 2009) are induced by TNFα, again suggesting that they function as a differentially regulated signaling module. OTULIN is subject to phosphorylation, acetylation, and ubiquitination in cells, and it will be interesting to study whether these modifications regulate its activity or function.

Overall, our data suggest that the identified DUB OTULIN is an antagonist of the LUBAC E3 ligase complex. Consistent with reported roles for Met1-polyUb, changing OTULIN expression affects LUBAC-mediated processes, including NF-κB signaling. Detailed genetic analysis will be necessary in order to under-

stand how LUBAC and OTULIN balance Met1-polyUb chains in vivo. This might confirm some reported roles and may reveal new cellular roles for this atypical Ub chain type.

#### **EXPERIMENTAL PROCEDURES**

#### **Identification of OTULIN**

FAM105B/OUTLIN was identified bioinformatically with generalized profile analysis, as described in the Extended Experimental Procedures.

## Cloning, Expression, and Purification

*FAM105B* was cloned from brain complementary DNA (Invitrogen), expressed in *E. coli* from pOPIN-F vector, and purified by anion exchange and gel filtration.

#### **Crystallization and Structure Determination**

Apo, SeMet-substituted, and mutant OTULIN were crystalized from 100 mM MES and imidazole, 30 mM MgCl<sub>2</sub>, 30 mM CaCl<sub>2</sub>, 10% (w/v) PEG 4k, and 20% glycerol (pH 6.5). The structure of apo OTULIN was determined by single anomalous dispersion, and subsequent structures were determined by molecular replacement.

#### **Qualitative DUB Linkage Specificity Assay**

Qualitative deubiquitination assays were performed as previously described (Komander et al., 2009).

#### **Binding Studies and DUB Kinetics**

Binding studies were performed as in Ye et al. (2011), and kinetic studies were performed as in Virdee et al. (2010) with FIAsH-tagged Met1-diUb variants.

## **Cellular Studies of OTULIN**

OTULIN and A20 were expressed from pOPIN-F or pcDNA4/TO/MRGS6H, HOIP, SHARPIN and HOIL-1L from pcDNA3.1, and GST-tagged NEMO were expressed from pEBG vectors. Stable T-REx 293 cell lines overexpressing pcDNA4/TO/MRGS6H-OTULIN or a pDEST30-EmGFP construct with an miRNA targeting the 3′ untranslated region of *FAM105B* were generated according to the manufacturer's protocol (Invitrogen). Knockdown analysis was performed in miRNA cell lines or with eight different siRNA sequences, as listed in the Extended Experimental Procedures.

#### NF-κB Activity Analysis

NF- $\kappa B$  activity was assessed by luciferase assays, for which cells were cotransfected with M3P sin rev  $\kappa B$  firefly and pRL-TK *Renilla* (Promega) luciferase plasmids by immunofluorescence with anti-p65 staining or by quantitative PCR, as described in the Extended Experimental Procedures. TNF $\alpha$  signaling was analyzed by western blotting with the antibodies listed in the Extended Experimental Procedures.

#### **ACCESSION NUMBERS**

Coordinates and structure factors have been deposited in the Protein Data Bank and can be found at accession numbers 3ZNV (WT OTULIN apo), 3ZNX (OTULIN apo D336A), and 3ZNZ (OTULIN-Met1-diUb).

# SUPPLEMENTAL INFORMATION

Supplemental Information includes Extended Experimental Procedures, six figures, and one table and can be found with this article online at http://dx.doi.org/10.1016/j.cell.2013.05.014.

#### **ACKNOWLEDGMENTS**

We would like to thank S. McLaughlin, R. Williams, A. Finch, F. Randow, G. Murshudov (Medical Research Council [MRC] Laboratory of Molecular Biology), G. Praefcke (University of Cologne), and members of the D. Komander lab for advice, reagents, and critical comments on the manuscript.

Liposome reagent for Jurkat T cell transfection was a kind gift of Silence Therapeutics, Berlin. This work was supported by the MRC (U105192732 to D. Komander), the European Research Council (309756 to D. Komander), the European Molecular Biology Organization Young Investigator program (D.K.), the Lister Institute for Preventive Medicine (D. Komander), the German Research Foundation (DFG Priority Programme SPP1365 to K.H. and D. Krappmann), the Novo Nordisk Foundation (M.G.H.), and a Steno Fellowship from the Danish Council for Independent Research (M.G.H.). Crystallographic data were collected at the European Synchrotron Radiation Facility at beam lines ID14-4 and ID23-1 and at Diamond Light Source beam line

Received: March 1, 2013 Revised: April 3, 2013 Accepted: May 6, 2013 Published: June 6, 2013

#### **REFERENCES**

Amerik AYu, Swaminathan, S., Krantz, B.A., Wilkinson, K.D., and Hochstrasser, M. (1997). In vivo disassembly of free polyubiquitin chains by yeast Ubp14 modulates rates of protein degradation by the proteasome. EMBO J. 16, 4826-4838.

Behrends, C., and Harper, J.W. (2011). Constructing and decoding unconventional ubiquitin chains. Nat. Struct. Mol. Biol. 18, 520-528.

Boisson, B., Laplantine, E., Prando, C., Giliani, S., Israelsson, E., Xu, Z., Abhyankar, A., Israël, L., Trevejo-Nunez, G., Bogunovic, D., et al. (2012). Immunodeficiency, autoinflammation and amylopectinosis in humans with inherited HOIL-1 and LUBAC deficiency. Nat. Immunol. 13, 1178-1186.

Borodovsky, A., Ovaa, H., Kolli, N., Gan-Erdene, T., Wilkinson, K.D., Ploegh, H.L., and Kessler, B.M. (2002). Chemistry-based functional proteomics reveals novel members of the deubiquitinating enzyme family. Chem. Biol. 9, 1149-1159.

Bucher, P., Karplus, K., Moeri, N., and Hofmann, K. (1996). A flexible motif search technique based on generalized profiles. Comput. Chem. 20, 3-23.

Damgaard, R.B., Nachbur, U., Yabal, M., Wong, W.W.-L., Fiil, B.K., Kastirr, M., Rieser, E., Rickard, J.A., Bankovacki, A., Peschel, C., et al. (2012). The ubiquitin ligase XIAP recruits LUBAC for NOD2 signaling in inflammation and innate immunity. Mol. Cell 46, 746-758.

Edelmann, M.J., Iphöfer, A., Akutsu, M., Altun, M., di Gleria, K., Kramer, H.B., Fiebiger, E., Dhe-Paganon, S., and Kessler, B.M. (2009). Structural basis and specificity of human otubain 1-mediated deubiquitination. Biochem. J. 418, 379-390

Faesen, A.C., Luna-Vargas, M.P.A., Geurink, P.P., Clerici, M., Merkx, R., van Dijk, W.J., Hameed, D.S., El Oualid, F., Ovaa, H., and Sixma, T.K. (2011). The differential modulation of USP activity by internal regulatory domains, interactors and eight ubiquitin chain types. Chem. Biol. 18, 1550-1561.

Frias-Staheli, N., Giannakopoulos, N.V., Kikkert, M., Taylor, S.L., Bridgen, A., Paragas, J., Richt, J.A., Rowland, R.R., Schmaljohn, C.S., Lenschow, D.J., et al. (2007). Ovarian tumor domain-containing viral proteases evade ubiquitinand ISG15-dependent innate immune responses. Cell Host Microbe 2,

Gerlach, B., Cordier, S.M., Schmukle, A.C., Emmerich, C.H., Rieser, E., Haas, T.L., Webb, A.I., Rickard, J.A., Anderton, H., Wong, W.W.-L., et al. (2011). Linear ubiquitination prevents inflammation and regulates immune signalling. Nature 471. 591-596.

Haas, T.L., Emmerich, C.H., Gerlach, B., Schmukle, A.C., Cordier, S.M., Rieser, E., Feltham, R., Vince, J., Warnken, U., Wenger, T., et al. (2009). Recruitment of the linear ubiquitin chain assembly complex stabilizes the TNF-R1 signaling complex and is required for TNF-mediated gene induction. Mol. Cell 36, 831-844.

Hayden, M.S., and Ghosh, S. (2008). Shared principles in NF-kappaB signaling. Cell 132, 344-362.

Hershko, A., and Ciechanover, A. (1998). The ubiquitin system. Annu. Rev. Biochem. 67, 425-479.

Hymowitz, S.G., and Wertz, I.E. (2010). A20: from ubiquitin editing to tumour suppression. Nat. Rev. Cancer 10, 332-341.

Ikeda, F., Deribe, Y.L., Skånland, S.S., Stieglitz, B., Grabbe, C., Franz-Wachtel, M., van Wijk, S.J.L., Goswami, P., Nagy, V., Terzic, J., et al. (2011). SHARPIN forms a linear ubiquitin ligase complex regulating NF-κB activity and apoptosis. Nature 471, 637-641.

Juang, Y.-C., Landry, M.-C., Sanches, M., Vittal, V., Leung, C.C.Y., Ceccarelli, D.F., Mateo, A.-R.F., Pruneda, J.N., Mao, D.Y.L., Szilard, R.K., et al. (2012). OTUB1 co-opts Lys48-linked ubiquitin recognition to suppress E2 enzyme function. Mol. Cell 45, 384-397.

Karin, M., and Ben-Neriah, Y. (2000). Phosphorylation meets ubiquitination: the control of NF-[kappa]B activity. Annu. Rev. Immunol. 18, 621-663.

Kayagaki, N., Phung, Q., Chan, S., Chaudhari, R., Quan, C., O'Rourke, K.M., Eby, M., Pietras, E., Cheng, G., Bazan, J.F., et al. (2007). DUBA: a deubiquitinase that regulates type I interferon production. Science 318, 1628-1632.

Kirisako, T., Kamei, K., Murata, S., Kato, M., Fukumoto, H., Kanie, M., Sano, S., Tokunaga, F., Tanaka, K., and Iwai, K. (2006). A ubiquitin ligase complex assembles linear polyubiquitin chains. EMBO J. 25, 4877-4887.

Komander, D., and Rape, M. (2012). The ubiquitin code. Annu. Rev. Biochem. 81, 203-229.

Komander, D., Reves-Turcu, F., Licchesi, J.D.F., Odenwaelder, P., Wilkinson, K.D., and Barford, D. (2009). Molecular discrimination of structurally equivalent Lys 63-linked and linear polyubiquitin chains. EMBO Rep. 10, 466-473.

Kulathu, Y., and Komander, D. (2012). Atypical ubiquitylation - the unexplored world of polyubiquitin beyond Lys48 and Lys63 linkages. Nat. Rev. Mol. Cell Biol. 13, 508-523.

Licchesi, J.D.F., Mieszczanek, J., Mevissen, T.E.T., Rutherford, T.J., Akutsu, M., Virdee, S., El Oualid, F., Chin, J.W., Ovaa, H., Bienz, M., and Komander, D. (2012). An ankyrin-repeat ubiquitin-binding domain determines TRABID's specificity for atypical ubiquitin chains. Nat. Struct. Mol. Biol. 19, 62-71.

Matsumoto, M.L., Dong, K.C., Yu, C., Phu, L., Gao, X., Hannoush, R.N., Hymowitz, S.G., Kirkpatrick, D.S., Dixit, V.M., and Kelley, R.F. (2012). Engineering and structural characterization of a linear polyubiquitin-specific antibody. J. Mol. Biol. 418, 134-144.

Mevissen, T.E., Hospenthal, M.K., Geurink, P.P., Elliott, P.R., Akutsu, M., Arnaudo, N., Ekkebus, R., Kulathu, Y., Wauer, T., El Oualid, F., et al. (2013). OTU Deubiquitinases Reveal Mechanisms of Linkage Specificity and Enable Ubiquitin Chain Restriction Analysis. Cell 154. Published online July 3, 2013. 10.1016/j.cell.2013.05.046.

Murshudov, G.N., Skubák, P., Lebedev, A.A., Pannu, N.S., Steiner, R.A., Nicholls, R.A., Winn, M.D., Long, F., and Vagin, A.A. (2011). REFMAC5 for the refinement of macromolecular crystal structures. Acta Crystallogr. D Biol. Crystallogr. 67, 355-367.

Nakada, S., Tai, I., Panier, S., Al-Hakim, A., Iemura, S.-I., Juang, Y.-C., O'Donnell, L., Kumakubo, A., Munro, M., Sicheri, F., et al. (2010). Non-canonical inhibition of DNA damage-dependent ubiquitination by OTUB1. Nature 466, 941-946.

Ozkaynak, E., Finley, D., and Varshavsky, A. (1984). The yeast ubiquitin gene: head-to-tail repeats encoding a polyubiquitin precursor protein. Nature 312,

Rahighi, S., Ikeda, F., Kawasaki, M., Akutsu, M., Suzuki, N., Kato, R., Kensche, T., Uejima, T., Bloor, S., Komander, D., et al. (2009). Specific recognition of linear ubiquitin chains by NEMO is important for NF-kappaB activation. Cell

Smit, J.J., Monteferrario, D., Noordermeer, S.M., van Dijk, W.J., van der Reijden, B.A., and Sixma, T.K. (2012). The E3 ligase HOIP specifies linear ubiquitin chain assembly through its RING-IBR-RING domain and the unique LDD extension. EMBO J. 31, 3833-3844.

Stieglitz, B., Morris-Davies, A.C., Koliopoulos, M.G., Christodoulou, E., and Rittinger, K. (2012). LUBAC synthesizes linear ubiquitin chains via a thioester intermediate. EMBO Rep. 13, 840-846.

Sun, S.-C. (2010). CYLD: a tumor suppressor deubiquitinase regulating NF-kappaB activation and diverse biological processes. Cell Death Differ.

Tokunaga, F., and Iwai, K. (2012). LUBAC, a novel ubiquitin ligase for linear ubiquitination, is crucial for inflammation and immune responses. Microbes Infect. 14, 563-572.

Tokunaga, F., Sakata, S.-I., Saeki, Y., Satomi, Y., Kirisako, T., Kamei, K., Nakagawa, T., Kato, M., Murata, S., Yamaoka, S., et al. (2009). Involvement of linear polyubiquitylation of NEMO in NF-kappaB activation. Nat. Cell Biol. 11, 123-132.

Tokunaga, F., Nakagawa, T., Nakahara, M., Saeki, Y., Taniguchi, M., Sakata, S.-I., Tanaka, K., Nakano, H., and Iwai, K. (2011). SHARPIN is a component of the NF-κB-activating linear ubiquitin chain assembly complex. Nature 471, 633-636.

van Wijk, S.J.L., Fiskin, E., Putyrski, M., Pampaloni, F., Hou, J., Wild, P., Kensche, T., Grecco, H.E., Bastiaens, P., and Dikic, I. (2012). Fluorescence-based sensors to monitor localization and functions of linear and K63-linked ubiquitin chains in cells. Mol. Cell 47, 797-809.

Virdee, S., Ye, Y., Nguyen, D.P., Komander, D., and Chin, J.W. (2010). Engineered diubiquitin synthesis reveals Lys29-isopeptide specificity of an OTU deubiquitinase. Nat. Chem. Biol. 6, 750-757.

Walczak, H., Iwai, K., and Dikic, I. (2012). Generation and physiological roles of linear ubiquitin chains. BMC Biol. 10, 23.

Wickliffe, K.E., Lorenz, S., Wemmer, D.E., Kuriyan, J., and Rape, M. (2011). The mechanism of linkage-specific ubiquitin chain elongation by a singlesubunit E2. Cell 144, 769-781.

Wiener, R., Zhang, X., Wang, T., and Wolberger, C. (2012). The mechanism of OTUB1-mediated inhibition of ubiquitination. Nature 483, 618-622.

Xu, M., Skaug, B., Zeng, W., and Chen, Z.J. (2009). A ubiquitin replacement strategy in human cells reveals distinct mechanisms of IKK activation by TNFalpha and IL-1beta. Mol. Cell 36, 302-314.

Ye, Y., Akutsu, M., Reyes-Turcu, F., Enchev, R.I., Wilkinson, K.D., and Komander, D. (2011). Polyubiquitin binding and cross-reactivity in the USP domain deubiquitinase USP21. EMBO Rep. 12, 350-357.